

# Chapter 6

## Photometric Correction (*PHOTOM*)

Non-linear photometric response and spatial sensitivity variations in the detectors are present in all raw data and must be taken into consideration before the data can be utilized for scientific purposes. In accounting for the detector response, the *PHOTOM* procedure converts raw data numbers (DN) into normalized flux numbers (FN) which are linearly related to the incident photon flux. *PHOTOM* is performed on a pixel-by-pixel basis in the two-dimensional raw image.

The *PHOTOM* procedure in NEWSIPS differs in two fundamental ways from the correction performed in IUESIPS. The Intensity Transfer Functions (ITFs) (i.e., graded ultraviolet floodlamp exposures used to linearize and normalize the camera response) are constructed in a manner which eliminates the necessity to resample, and consequently degrade, the data and preserves the inherent characteristics of the detector. In addition, a more precise image registration technique (Chapter 5) is used to align accurately the raw science data with the ITFs (Shaw 1990, De La Peña et al. 1990).

### 6.1 Construction of the ITFs

The modern epoch ITF series used for the Final Archive (LWP:1992, LWR:1983, and SWP:1985) were obtained in a closely monitored and stable satellite configuration such that any parameters known to affect the image quality (e.g., camera temperature) were carefully controlled. These improved acquisition procedures ensured that the constituent ITF images at each exposure level have little geometric distortion relative to each other. The ITFs for the Final Archive have been constructed in raw space with no attempt to align geometrically the images, because some smoothing of the ITF data is inherent in such an alignment. The raw images for each level were averaged on a pixel-by-pixel basis to form a mean level. If the intensity level of a pixel from one of the component images varied from the mean intensity value for that pixel by more than 2.5 sigma for the SWP and LWR ITFs and 1.4 sigma for the LWP 1992 ITF, the deviant pixel was excluded from the sum. In this way it was possible to use images with missing minor frames in the construction of the ITF. Each level of the ITF is constructed with at least 4 images; the null level was typically constructed with many

more images. The resulting ITF for each camera is a three-dimensional file of dimensions  $768 \times 768 \times 12$  pixels.

The lowest level of the ITF is a zero exposure or null level which is the background left by the standard camera flood/erase preparation procedure. Correspondingly, the highest level of the ITF has a long enough exposure time to allow the detector to achieve its saturation limit of 255 DN over a majority of the image. The intermediate ITF levels map the camera response through the mid-range of DN values. The 12 level ITF provides sufficient granularity in intensity to allow linear interpolation between the levels.

### 6.1.1 LWP ITF

The ITF originally acquired for the LWP camera in 1978–1980 was a “mini-ITF” with one image for most of the levels. These images were taken under widely varying spacecraft conditions, with some images taken during optimization testing when camera parameters were deliberately modified. The ITF taken in 1984 was taken under controlled conditions and the images are geometrically similar, allowing the construction of a raw space ITF. However, it was discovered during testing of this ITF that the LWP dataset of science images divide generally into two subgroups. Images taken before 1984 tend to have similar geometric distortions to one another, and images taken after 1984 tend to have similar geometric distortions, but the two subgroups are not geometrically similar to each other. Clearly, there was a discrete change in the camera operating parameters in 1984, possibly in the voltages set in the camera, but the information available via telemetry is not sufficient to identify the exact nature of the change. Unfortunately, images taken before the 1984 ITF (a very small percentage of the total LWP dataset) are geometrically similar to the LWP ITF (Epoch 1984). Images taken after the 1984 ITF are not well aligned with the 1984 ITF. This situation prompted the acquisition of a new ITF for the LWP camera in 1992.

The LWP ITF acquired in 1992 is virtually always better aligned in raw space with the science images acquired since 1984 than the 1984 ITF. However, the bimodal nature of the image distortion for the LWP camera manifested itself in the null images acquired for the 1992 ITF. The null level images formed two discrete groups. Approximately half the null images are geometrically similar to each other and form an internally consistent group (Null A). The other group of null images (Null B) are geometrically similar to each other in raw space, but the two groups are not sufficiently aligned geometrically to be co-added without loss of accuracy in *PHOTOM*. While somewhat more than half of the science images acquired with the LWP camera are better aligned with Null B than Null A, the intensity level of Null B is higher than that of Null A, resulting in the science data not being fully bracketed by the calibration ITF data in intensity when Null B is used. The Final Archive processing uses the 1992 LWP ITF constructed with Null A.

### 6.1.2 LWR ITF

As is the case with the LWP camera, two ITFs were acquired for the LWR. The first ITF (1978 epoch) was acquired with no constraints placed on camera temperature (THDA). Hence, a viable raw space ITF could not be constructed from the 1978-epoch dataset (i.e., the individual UV-Flood images in a given ITF level did not align geometrically with one another). The second ITF (1983 epoch) was taken under more controlled spacecraft conditions; however, an ITF constructed purely using the 1983-epoch images (LWR83R94A or ITF A) did not correlate well with pre-1984 science images. As a result, a “hybrid” 1983-epoch ITF (LWR83R96A or ITF B) was generated where all levels (except the null) of the ITF were constructed from UV-Flood images taken during the 1983 ITF acquisition and the null level is composed of six null images taken during the 1978–1983 time period. LWR science images show a marked bimodality as far as ITF preference is concerned. For the most part, the majority of low-dispersion images taken prior to 1984 tend to correlate well with ITF B; while images taken after this date register well with the ITF A.

LWR ITF selection in NEWSIPS low-dispersion processing is made on an image-by-image basis. Each low-dispersion LWR image is processed twice through the image registration (*CROSS-CORR*) step; once using ITF A and another time utilizing ITF B. NEWSIPS then chooses the ITF which yields a higher median cross-correlation coefficient for subsequent processing of the image. High-dispersion LWR images do not go through such a selection process; only ITF A is used. This is because no clear improvement in image quality was seen when using ITF B over ITF A in high dispersion.

### 6.1.3 SWP ITF

At the time of construction of the SWP ITF for use in the Final Archive, two ITF series had been acquired for that camera. The images that comprise the ITF acquired in 1978 were not acquired under stable spacecraft conditions and are geometrically dissimilar to each other. These images cannot be used to construct a raw space ITF, which requires minimal distortion among the images. The images acquired for the 1985 ITF comprise a geometrically homogeneous group. Therefore, the images acquired for the 1985 ITF were used to construct the raw space ITF for the Final Archive processing. In 1992, a new ITF for the SWP camera was acquired, but there are no current plans for use of this ITF in the Final Archive processing.

### 6.1.4 Periodic Noise

All raw *IUE* images suffer from periodic noise (Nichols-Bohlin 1988, Shaw 1989) which is constant in raw space. The noise has been found to be multiplicative in nature and ranging from 1% to 8% in amplitude; however, the particular periodicities present and the amplitude of the noise are camera specific. Due to geometric distortion, the periodic noise in the ITF will not, in general, align with the noise present in the science image, and therefore, the periodic noise has been filtered from the ITF images using a Fourier-filtering technique. For

the SWP camera, noise spikes were filtered every 192 points in the line direction and every 16 points in the sample direction in frequency space. For the LWP camera, noise spikes were filtered every 12 points in the line direction and every 16 points in the sample direction. The noise features in the LWR camera are much larger (8%) than the other cameras; noise spikes every 192 points are filtered in both the line and sample directions.

## 6.2 Determination of the Effective Exposure Times

The effective exposure times for the 1983–1985 Epoch ITFs were derived by Imhoff (1984b and 1986), by De La Peña and Coulter (1996) for the 1992 Epoch LWP ITF, and by De La Peña for the LWR ITFs. During the creation of the 1983–1985 ITFs in their own geometric space for the NEWSIPS system, if additional images were deemed usable in contrast to those originally chosen by Imhoff, the effective exposure times were modified to reflect the use of additional images.

Table 6.1 lists the effective exposure times (FN exposure values) for each level of the ITFs used in the Final Archive. These exposure values have been normalized to an arbitrary scale such that the FN associated with the lowest level of an ITF is 0.0.

Table 6.1: ITF Effective Exposure Times (seconds)

ITF Level	SWP Epoch 1985	LWP Epoch 1992	LWR ITFA Epoch 1983	LWR ITFB Epoch 1983
1	0.000	0.000	0.000	0.000
2	32.919	38.750	35.880	35.607
3	67.946	78.737	72.974	72.425
4	104.147	121.868	91.067	89.708
5	131.397	168.958	125.213	125.621
6	166.296	200.756	156.510	162.627
7	223.034	237.941	193.275	198.780
8	269.680	278.107	245.053	254.362
9	340.471	341.073	283.705	288.706
10	408.490	396.582	320.355	325.599
11	473.749	483.497	385.554	401.720
12	575.995	561.518	471.557	490.480

## 6.3 Description of the Photometric Correction

The actual pixels *PHOTOM*ed in high dispersion reside within a region defined by edge-detection algorithms on raw, well-exposed UV Flood images. These pseudo-circular regions coincide with the target boundary. For low dispersion, only a diagonal swath of data encompassing both the large and small apertures, as well as a generous portion of the background, is *PHOTOM*ed.

The *PHOTOM* procedure accesses *explicitly* determined displacements between the raw science image and the ITF to align the two images and to convert the DN to FN. These displacements have been derived using the image registration technique as described in Chapter 5.

### 6.3.1 Determination of the ITF Pixels

Displacement vectors calculated in the *CROSS-CORR* step map each pixel in the raw science image to the geometric space of the ITF, where the final displacement coordinates are floating point coordinates. If the final coordinates for the science pixel are within 0.125 pixel (in either the line or sample direction) of the integer coordinates of an ITF pixel, the science image pixel is assumed to be coincident with the ITF pixel and the FN computed will be based upon data contributed only from the single ITF pixel. If the science image pixel is displaced by more than 0.125 pixel from the integer coordinates of any ITF pixel, the FN computed will be based upon data contributed from a  $4 \times 4$  matrix of ITF pixels surrounding the final position in question. Both of these scenarios are described in further detail in the next section.

### 6.3.2 Determination of the Flux Values

In contrast to the original IUESIPS *PHOTOM*, the raw DN values are converted to linearized (i.e., photometrically corrected) FN values directly from the effective exposure time associated with each level of the ITF. For a given pixel the FN associated with level  $i$  of the ITF is:

$$FN_i = T(i)$$

where  $T(i)$  is the effective exposure time in seconds for level  $i$ .

There are four basic methods for the determination of the FN of a raw science image pixel from a single ITF pixel (for the case where the displacement coordinates of the science image are  $\leq 0.125$  pixel from the ITF pixel coordinate). In the following discussion, let  $DN(ITF_1)$  represent the DN level of the relevant pixel in the first ITF level; let  $DN(ITF_{12})$  represent the DN level of the relevant pixel in the twelfth ITF level; let  $DN_{raw}$  represent the DN level of the science image pixel; and let  $DN_{sat}$  represent the DN level of saturation for the relevant pixel. Then the four alternatives are:

- **Fully calibrated data:** When  $DN(ITF_1) \leq DN_{raw} \leq DN(ITF_{12})$ , the FN is determined with a linear interpolation algorithm. The interpolation is performed between the two ITF levels that bound the input DN in intensity.
- **Saturated data:** When  $DN_{raw} \geq DN(ITF_{12})$  and  $DN_{raw} \geq DN_{sat}$ , the pixel is considered to be saturated and the FN is set to a constant (the FN value for the top level of the ITF; see Table 6.1).  $DN_{sat}$  has been determined on a pixel-by-pixel basis through analysis of the individual ITF curves and is defined to be the DN at which the slope of the ITF curve (DN versus exposure level) approaches zero. Since ITF curves vary considerably from pixel to pixel, the DN level corresponding to saturation varies from pixel to pixel. The flagging of saturated data is broken down into two separate cases; in either case, the FN for the pixel in question is set to the FN of the top level of the ITF:
  - Case 1:**  $DN_{raw} = DN(ITF_{12})$ . These pixels are flagged with the saturation flag of  $-1024$ .
  - Case 2:**  $DN_{raw} > DN(ITF_{12})$ . These pixels are flagged with both the saturation flag of  $-1024$  and a positive extrapolation flag of  $-256$ . In this instance, the assignment of an extrapolation flag serves only to identify the fact that the DN exceeds that of the top level of the ITF; no extrapolation of the FN data is performed.
- **Positively extrapolated data:** When  $DN_{raw} > DN(ITF_{12})$  and  $DN_{raw} < DN_{sat}$ , the FN is computed by a two-point extrapolation from the top two levels of the ITF. These pixels are flagged with the positive extrapolation flag of  $-256$ .
- **Negatively extrapolated data:** When  $DN_{raw} < DN(ITF_1)$ , the FN is computed with a two-point extrapolation from the bottom two levels of the ITF. However, the pixel is only flagged with an indication of negative extrapolation if the extrapolation is considered excessive. For this purpose, a “negative extrapolation reference image” has been created by determining the 50% intensity level of the ITF null image, and smoothing these data with a 5-point boxcar in two-dimensions. Consequently, negative extrapolations are only considered excessive and flagged if  $DN_{raw} < DN_{neg. ext. ref. image}$ . Excessive negative extrapolations are flagged with a value of  $-128$ .

When there is significant misalignment ( $>0.125$  pixel) between the raw science image and the ITF, a  $4 \times 4$  matrix of ITF pixels surrounding the location in question is used to compute the relevant FN. Using the raw science image DN, an FN value is computed at each of the  $4 \times 4$  locations in the matrix, using the above described single-pixel scenarios. The median FN in the matrix is computed, and then deviant values are eliminated from the FN matrix and replaced with the median FN. FN values are considered to be deviant if they are different from the median by more than 100 FN. Once the FN matrix has been defined and deviant values replaced, the matrix is fit with a spline surface which is evaluated at the final coordinate location desired for the final FN value.

The FNs determined during the *PHOTOM* procedure have values which range between  $\pm 1024$ . Any FN values originally exceeding these limits are clipped and set to the respective limit value.

## 6.4 Associated $\nu$ Flags and Reference Images

### 6.4.1 Non-photometrically Corrected Image Regions

As discussed in Chapter 6.3, the regions defined for *PHOTOM* either reside within an approximately circular boundary for high dispersion, or a diagonal swath encompassing the location of both apertures and a large area of background for low dispersion. All pixel locations which do not reside within these defined boundaries are not *PHOTOM*ed and are flagged as  $-16384$ .

### 6.4.2 Warning Track

In order to alert the user that data being analyzed are spatially close to the edge of the *PHOTOM* region and/or near the target ring, a warning zone approximately five pixels deep has been established on the *PHOTOM*ed data side of the boundary. Pixel locations determined to be in the warning track are flagged as  $-512$ .

### 6.4.3 ITF Artifacts

#### 6.4.3.1 Permanent Artifacts and Reseaux

The permanent ITF artifacts have been cataloged and both the artifacts and reseaux have been removed from the ITF images with a bi-linear interpolation scheme. The location of the specific pixels affected by either an artifact or reseau mark have been preserved in an ITF-dependent “permanent blemish” reference image. This image is used in the pipeline processing during the *PHOTOM* step to flag pixels in the science image whose location is coincident to those of the ITF blemishes. The  $\nu$  flag values corresponding to permanent ITF artifacts and reseaux are  $-2048$  and  $-4096$ , respectively. Because the ITF has been spatially interpolated in these regions, the accuracy of *PHOTOM* is somewhat degraded in the vicinity of the pertinent artifacts and reseaux.

#### 6.4.3.2 The 1515Å Artifact

Analyses of presumably featureless SWP spectral data of white dwarfs have revealed a distinctive absorption artifact at 1515Å. Although this “feature” is now known to be present in a variety of the SWP spectra, its presence in the featureless white dwarf spectra analyzed for flux calibration studies was the catalyst for further investigation and allowed the absolute determination of this “feature” as an artifact (De La Peña 1992).

Figure 6.1 is a plot of the SWP spectrum of the white dwarf, G191-B2B, a featureless continuum source. The spectra were produced with the standard extraction method of the NEWSIPS image processing system, a Signal Weighted Extraction Technique (*SWET*).

Upon further investigation, the 1515Å feature was found to be present in both NEWSIPS and IUESIPS data. Recall that NEWSIPS is using a *SWET* extraction and the SWP ITF (Epoch 1985) was constructed in raw space. IUESIPS uses a standard boxcar extraction and the SWP ITF (Epoch 1978) was constructed in geometrically corrected space. Therefore, this artifact is independent of the extraction method, and both the ITF epoch and creation method. Despite the major differences in the image processing techniques employed by the two systems, the feature is apparent in both datasets. In addition, not only is this artifact found in these recently obtained white dwarf observations (1991), but it also can be found in extracted spectra acquired as early as 1978.

Using the data from a specific SWP image in which this absorption feature is present, the vector displacement information was used to trace the pixels in the extracted/resampled (MX/SI) images back to the linearized and raw images (LI and RI, respectively), and ultimately back to the ITF. There appears to be a group of “lazy” pixels in the ITF at the computed location. These pixels lack sensitivity in the lowest levels of the ITF in that they require more illumination than their neighbors before they “react.” Unfortunately, there are several adjacent pixels along the edge of the low-dispersion spectral swath which appear to be less sensitive than the neighboring pixels at low illumination levels. It is simply an unfortunate circumstance that these pixels reside along the edge of the spectral swath, and therefore, manifest themselves as a flux deficit in the extracted data. Because of the difficulty in accurately identifying the pixels contributing to the 1515Å artifact due to the variable placement of the spectrum on the image, this artifact is not flagged.

## 6.5 *PHOTOM* Output

The low-/high-dispersion LI FITS files (LILO/LIHI) are the main output data product produced during the *PHOTOM* stage of image processing. This file contains the LI and associated  $\nu$  flag (LF) data. For both low and high dispersion, the LI and LF arrays are full  $768 \times 768$  images. The LI contains FN values in RI space for the data which have been *PHOTOM*ed. Since the LI was created by overwriting a copy of the RI, the remainder of the data in the LI frame outside the *PHOTOM* region are the raw data scaled down by a factor of 32. The LF contains the *PHOTOM*  $\nu$  flag error conditions which have been combined with the conditions determined during the raw image screening portion of image processing. The intensity data (LI) are output as the FITS primary array, and the associated  $\nu$  flags (LF) are output as the corresponding FITS image extension to the LILO/LIHI.

The *PHOTOM* module writes the following information to the HISTORY portion of the image label:

- ITF used by *PHOTOM* (camera and ITF acquisition epoch),
- mean THDA of ITF,



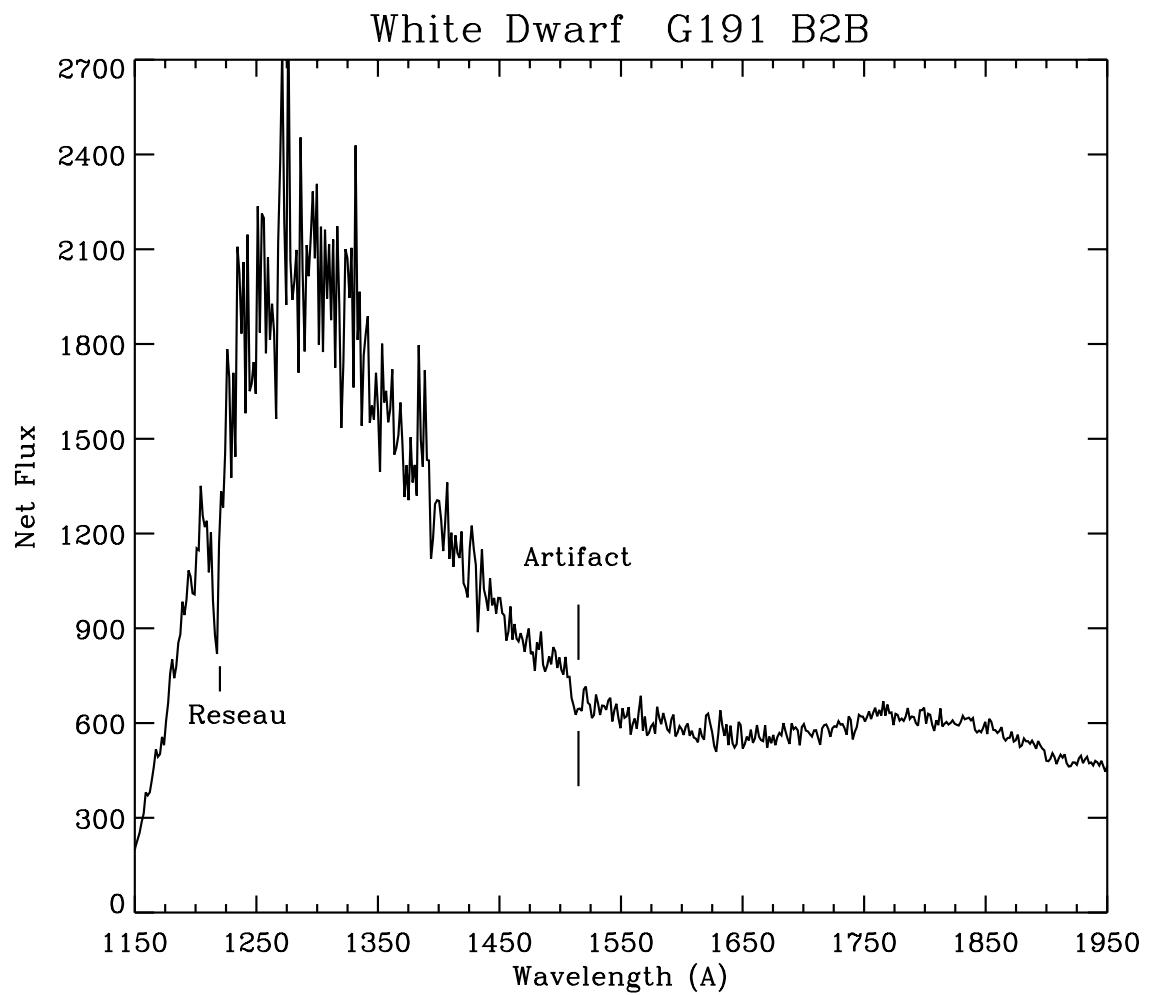


Figure 6.1: White Dwarf SWP spectra showing the 1515Å artifact.

- ITF UVC voltage, UV flood wavelength, ITF SEC voltage, and
- ITF characteristics and construction date.